Study On Low Power Novel 12-Pole E-Type Tooth Hybrid Magnetic Bearing

Jiarui Li *, Dong Jiang **, Tianci Sun **
* China-EU Institute for Clean and Renewable Energy，Huazhong University of Science and Technology
Wuhan 430074, Hubei province，China
E-mail: m202271346@hust.edu.cn
** School of Electrical and Electronic Engineering, Huazhong University of Science and Technology
Wuhan 430074, Hubei province，China

Abstract
This paper presents a novel 12-pole E-type tooth hybrid magnetic bearing (HMB) designed for high-efficiency and low-power suspension applications. The proposed HMB integrates sheet-type NdFe35SH permanent magnets with a symmetrical E-shaped stator structure to reduce energy consumption while maintaining high levitation precision. An equivalent magnetic circuit model is established to analyze the flux distribution and force generation mechanisms. Finite element simulations confirm that the magnetic force varies linearly with current, and a prototype system was built to experimentally evaluate performance. Test results show that the rotor displacement remains within ±15 μm up to 3000 rpm, and the total power loss is reduced by over 90% compared to conventional fully active magnetic bearings. These findings demonstrate the feasibility of the proposed design in compact and energy-sensitive systems such as kitchen ventilation motors and flywheel energy storage devices.

Keywords: Hybrid Magnetic Bearing, Low Power, E-type Tooth,12-Pole, Magnetic Circuit Design

1. Introduction

Magnetic bearings are widely recognized for their advantages in high-speed, non-contact, and low-maintenance applications(Maslen & Schweitzer, 2009; Schweitzer, 1978). They are particularly attractive in energy-efficient systems such as clean energy generators, precision machinery, and industrial ventilation equipment (Allaire et al., n.d.). Among them, active magnetic bearings (AMBs) have demonstrated excellent dynamic performance and stability (Zhou & Li, 2016). However, the continuous electromagnetic excitation required by AMBs often leads to high power consumption, which limits their applicability in long-duration and energy-sensitive scenarios (Zheng et al., 2017).

Hybrid magnetic bearings (HMBs), which combine permanent magnet (PM) biasing with active electromagnetic control, have been proposed to address this issue (Wei et al., 2012; Zhang et al., 2021). In an HMB, the PMs provide the baseline magnetic field required for levitation, thereby reducing the current demand and copper losses in the control coils. Previous studies have explored multiple hybrid configurations to improve force density and reduce power loss. For instance, Sun et al. (Sun et al., 2017) proposed a four-degree-of-freedom HMB for momentum control, while Ye et al. (Ye & Le, 2020) developed a homopolar design with enhanced flux efficiency. However, these designs still face challenges including strong magnetic coupling, high complexity, and lack of full-scale experimental validation (Garcia et al., 2009; Qinghai et al., 2011).

To address these limitations, this paper proposes a novel 12-pole E-type tooth hybrid magnetic bearing featuring symmetric structure, low leakage flux, and high-power efficiency. By embedding NdFe35SH permanent magnets between E-type poles and optimizing the magnetic path, the bearing ensures highly linear force-current behavior. Simulations show that the total power loss is reduced by approximately one-third compared to conventional AMBs. Furthermore, experimental tests demonstrate that the rotor displacement remains within ±15 μm at 3000 rpm, achieving suspension accuracy comparable to active systems. This work contributes a validated hybrid bearing architecture that achieves both energy-saving and high-performance goals. It is suitable for applications such as kitchen ventilation fans, flywheel systems, and compact high-speed rotating machinery.

2. Structural and Magnetic Circuit Analysis of the Novel 12-Pole E-Type Tooth HMB

The proposed hybrid magnetic bearing (HMB) features four symmetrically distributed E-type magnetic poles arranged circumferentially around the stator. This structural arrangement inherently isolates each pole magnetically, effectively eliminating coupling between adjacent poles at the design level.

Each E-type pole consists of a central main tooth and two side auxiliary teeth, forming a claw-like geometry. As shown in Fig. 1, a sheet-shaped NdFe35SH permanent magnet is embedded within the main tooth of each pole, providing a stable bias magnetic flux for the magnetic circuit.

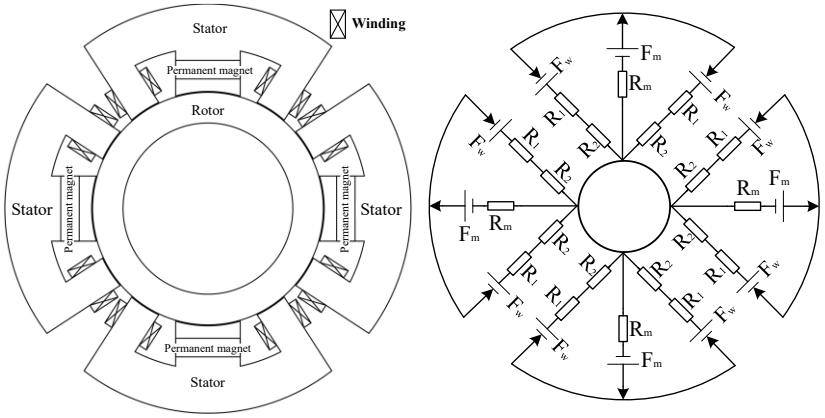

Fig. 1 Schematic diagram of the structure of the HMB and its equivalent magnetic circuit

The rotor, made of laminated silicon steel, is suspended concentrically within the stator with a 0.5 mm air gap. Control windings are placed on the auxiliary teeth and driven in a differential configuration to produce radial electromagnetic forces for dynamic adjustment.

This structure achieves both low power consumption and high levitation precision through the combined action of permanent magnets and active control. To further analyze the electromagnetic mechanism, an equivalent magnetic circuit model based on a single E-type tooth is established as follows.

The equivalent magnetic circuit model includes the magnetomotive force (MMF) provided by the permanent magnet F_m, the coil-generated MMF (F_w), and the reluctances of the permanent magnet (R_m), the small tooth air gap (R_1), and the large tooth air gap (R_2). Magnetic leakage and eddy current losses are neglected in this analysis.

Due to the symmetrical structure of the stator in the 12-pole E-shaped tooth hybrid magnetic bearing, when calculating parameters such as magnetic flux, it is only necessary to analyze the magnetic circuit model in a single degree of freedom. The single-degree-of-freedom equivalent magnetic circuit of the 12-pole E-shaped tooth hybrid magnetic bearing is shown in the Fig. 2.

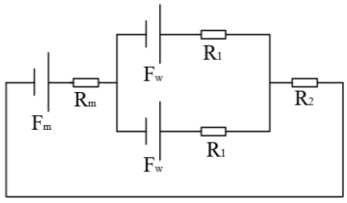

Fig. 2 Simplified Equivalent Magnetic Circuit Diagram

Magnetic Flux in the Main Tooth

$$\phi_2 = \frac{F_m + F_w}{R_m + (R_1 \,/\!/\, R_1) + R_2} \tag{1}$$

Magnetic Flux in the Auxiliary Tooth

$$\phi_1 = \frac{1}{2}\phi_2 \tag{2}$$

Magnetic Reluctance of the Permanent Magnet

$$R_m = \frac{l}{\mu_0 A_2} \tag{3}$$

Magnetic Reluctance of the Small Tooth Air Gap

$$R_1 = \frac{\delta}{\mu_0 A_1} \tag{4}$$

Magnetic Reluctance of the Large Tooth Air Gap

$$R_2 = \frac{\delta}{\mu_0 A_2} \tag{5}$$

Magnetic Flux in the Small Tooth Air Gap

$$B_1 = \frac{\phi_1}{A_1} \tag{6}$$

Magnetic Flux in the Large Tooth Air Gap

$$B_2 = \frac{\phi_2}{A_2} \tag{7}$$

Based on the principles of field energy and virtual displacement, the magnetic tensile force exerted by the Y-direction E-Type tooth hybrid magnetic bearing stator on the rotor is derived as:

$$W = \frac{1}{2} HBV \tag{8}$$

$$f_E = \frac{\partial W}{\partial s} = 2 f_1 \cos\alpha + f_2 = \frac{B_1^2 A_1}{\mu_0} \cos\alpha + \frac{1}{2} \frac{B_2^2 A_2}{\mu_0} \tag{9}$$

This magnetic circuit formulation provides the theoretical foundation for subsequent simulation and experimental validation.

3. Parameter Design and Simulation Verification

Based on the electromagnetic force requirement and structural constraints, the geometric parameters of the 12-pole E-type hybrid magnetic bearing were designed and optimized. The design target is to generate at least 470 N of radial electromagnetic force under a maximum excitation current of 10 A. This is required not only to support the rotor under normal levitation conditions, but also to provide sufficient differential force to counteract the unbalanced magnetic pull caused by permanent magnet bias under eccentric rotor positions. As shown in Tab. 1, key dimensional parameters include a rotor outer diameter of 62 mm, stator inner diameter of 63 mm, small and large tooth widths of 8 mm and 16 mm respectively, and an air gap of 0.5 mm.

Table1 Basic size parameters of the new twelve-pole E-tooth hybrid magnetic bearing

parameters	Value
rotor outer diameter d_1	62mm
air gap s	0.5mm
inner diameter of stator D_0	63mm
Stator median diameter D_1	136mm
stator outer diameterD_2	168mm
Large-toothed magnetic pole width t_2	16mm
Width of the small tooth magnetic pole t_1	8mm
Extreme boot height c	16mm
axial length b	30mm
Magnetic pole height h	36.5mm

The permanent magnet in each E-tooth is a key component for generating bias flux and reducing the need for external excitation. To ensure thermal reliability under high-frequency operation, a high-coercivity NdFe35SH material was selected, with a maximum working temperature of 150 °C. The magnet thickness was set to 2 mm, and the width to 15 mm, which provides sufficient magnetomotive force without excessively increasing reluctance. Since the control coil excitation shares the same magnetic path through the main tooth and magnet, the material's magnetic permeability and demagnetization tolerance must be carefully considered. This design balances MMF, reluctance, flux uniformity, and manufacturability, enabling stable operation under thermal and dynamic loads. The winding design is based on the requirement that the magnetic bearing must compensate for both rotor gravity and eccentricity-induced unbalanced

magnetic force. The rotor weighs 7 kg, producing approximately 70 N of gravitational force. At 0.25 mm eccentricity, the imbalance force reaches 92 N. To ensure sufficient recentering capability, each E-tooth must generate at least 162 N of electromagnetic force. The required ampere-turns are about 1080; 1200 ampere-turns are selected for margin. Assuming a 10 A max current, the coil uses 120 turns of 1 mm diameter copper wire, with acceptable fill factor.

Finite element simulations were conducted in Ansys Maxwell to verify the magnetic field distribution and force-current characteristics under both 5 A and 10 A excitation conditions. As shown in Fig. 3, he results show that the magnetic flux density in the small and large tooth air gaps reached 0.77 T/0.85 T at 5 A and 1.08 T/1.18 T at 10 A, without significant magnetic saturation.

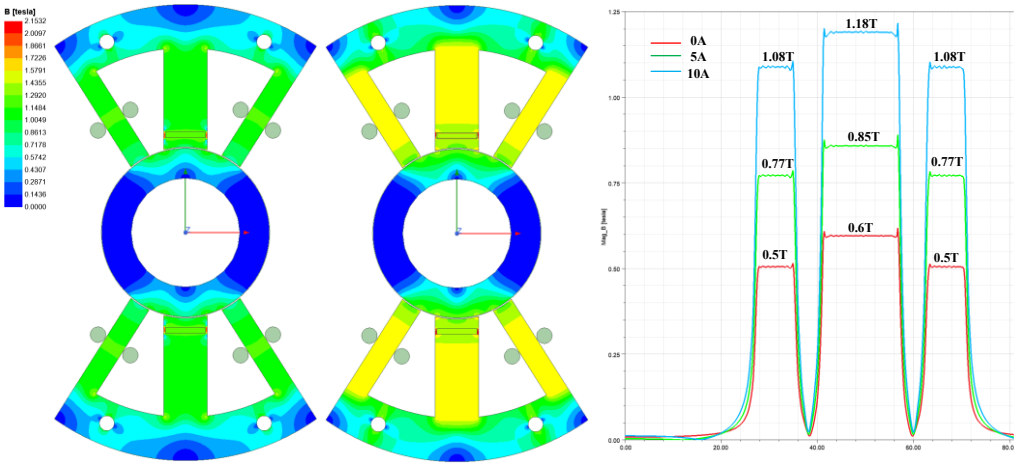

Fig. 3 The magnetic flux density contour and air-gap flux distribution plots of HMB

As shown in Figure 4, the electromagnetic force generated by a single E-tooth was found to increase approximately linearly with current, reaching 475.5 N at 10 A, which is consistent with the analytical model.

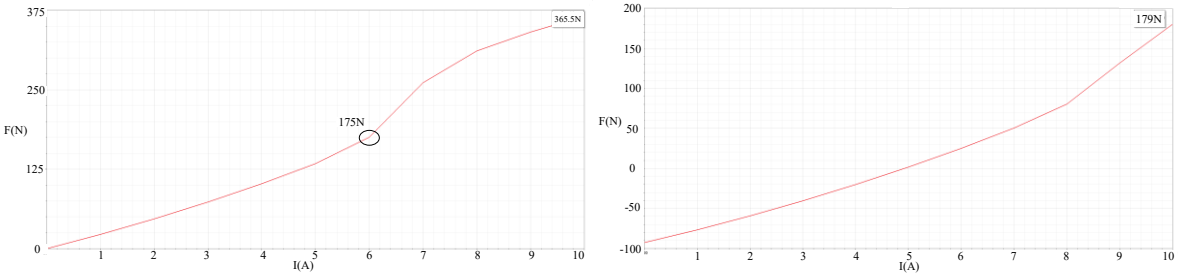

Fig. 4 The electromagnetic force versus current curve of a single E-pole.

To further evaluate the bearing's recentering ability, simulations were performed under an eccentric condition where the rotor was displaced by 0.25 mm, creating an air gap asymmetry of 0.25 mm and 0.75 mm on opposite sides. Under this condition, an unbalanced magnetic force of approximately 92 N was observed between the opposing poles. At 10 A excitation current, each E-tooth generated 179 N of radial force, which is sufficient to overcome both the eccentricity-induced imbalance and the gravitational load of the 7 kg rotor.

These results demonstrate that the designed HMB has strong recentering capability and stability under worst-case displacement conditions.

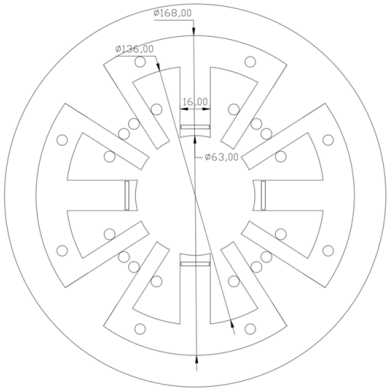

Fig. 5 radial dimensions of the low-power novel twelve-pole E-type tooth hybrid magnetic bearing

Table2 final geometric and electromagnetic design parameters of the new twelve-pole E-tooth HMB

Parameters	Value
rotor outer diameter d_1	62mm
air gap s	0.5mm
inner diameter of stator D_0	63mm
Stator median diameter D_1	136mm
stator outer diameter D_2	168mm
Large-toothed magnetic pole width t_2	16mm
Width of the small tooth magnetic polet_1	8mm
Extreme boot height c	16mm
Magnetic pole height h	36.5mm
The Angle between the large and small teeth α	33°
axial length b	30mm
Radial length of the permanent magnet l	2mm
Width of permanent magnet t_m	15mm
Permanent magnet type model	Ndfe35SH
Max working temperature	150℃
Turns per coil	120

The final geometric and electromagnetic design parameters are summarized in Table 2. These values serve as the basis for prototype fabrication and experimental validation. A schematic diagram of the bearing structure and radial dimensions is shown in Fig. 5. These results confirm the correctness of the geometric and excitation design, and provide a solid foundation for prototype fabrication and experimental validation in the following section.

4. Experimental Platform and Results

To validate the simulation results and assess real-world performance, a prototype of the proposed 12-pole E-type hybrid magnetic bearing was fabricated and tested on a self-built experimental platform. As shown in Fig. 6, the platform includes a 1 kW servo motor (rated at 3000 rpm), rotor assembly, dual-axis position sensors, two HMB stators, and an AMB controller with feedback current regulation.

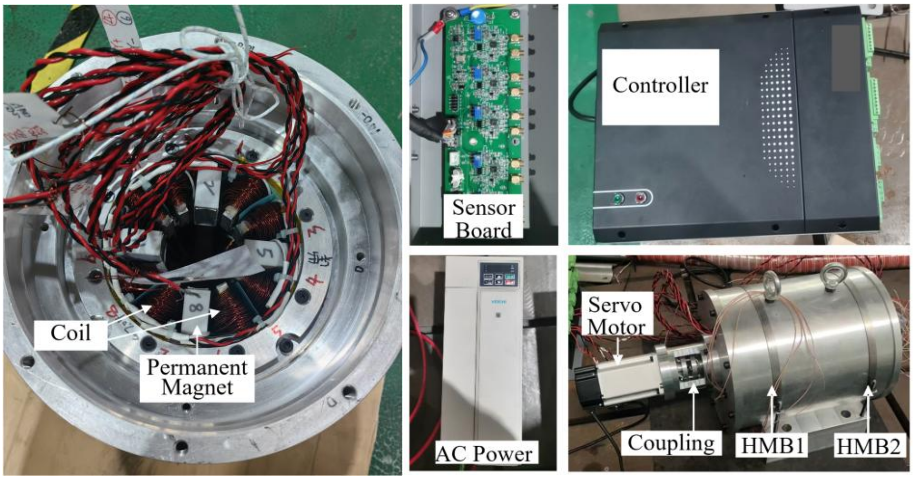

Fig. 6 Actual prototype and experimental platform

After the rotor floats, the servo motor drives the rotor to rotate through a coupling. The servo motor in the experiment adopts sensorless control and is driven by a frequency converter to a rated speed of 3000rpm. Figure 7 records the displacement and current waveform of the four degrees of freedom during the acceleration process. It can be seen that during the acceleration process, the displacement fluctuation is less than 15um, and the current ripple is less than ± 1A, indicating good performance of the control system.

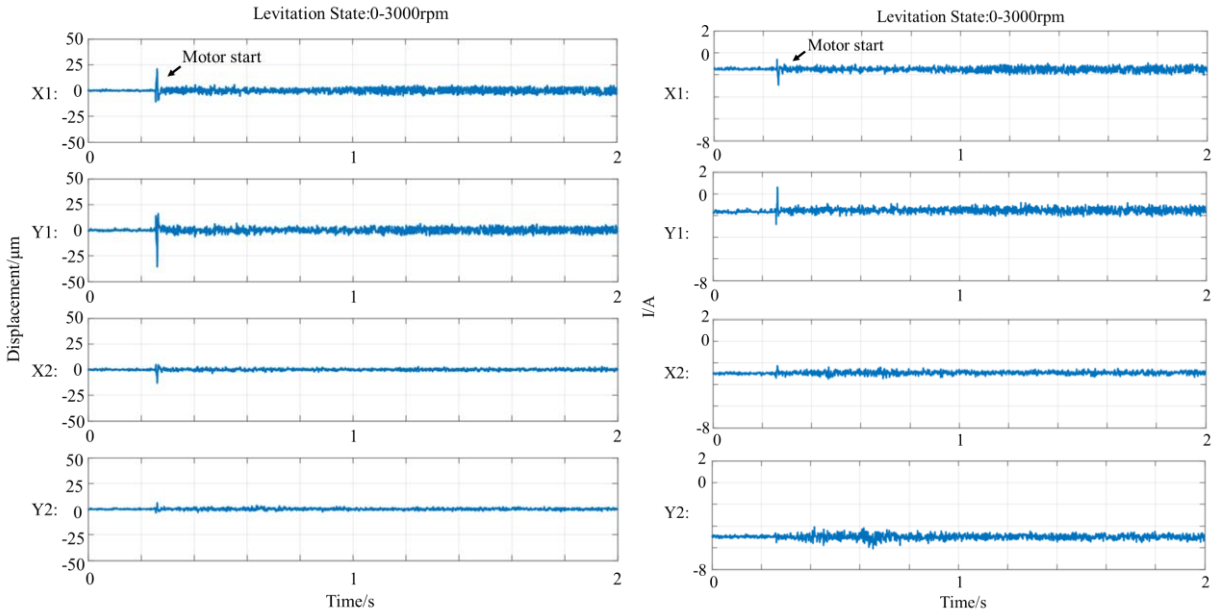

Fig. 7 Measured displacement and current waveforms in the X_1, Y_1, X_2, and Y_2 directions.

To evaluate power efficiency, steady-state control currents were recorded and analyzed. In hybrid magnetic bearings, the upper and lower windings of the same degree of freedom are often connected in reverse parallel to generate magnetic fields in opposite directions for differential control. After measurement, the resistance of each winding of the magnetic bearing is approximately 430 Ω. The steady-state control currents in all directions are X_1:-1.34A, Y_1: -1.46A, X_2: -2.93A, Y_2: -5.16A. If we consider the current to be evenly distributed, the actual current in two windings with the same degree of freedom is: X_1:0.67A, Y_1:0.73A, X_2:1.46A, Y_2:2.58A as shown in Tab. 3. If the copper loss generated by the current in the winding is used as the main power loss of the magnetic bearing, the total power loss $P\approx8.4W$.

Table3 Average current in each direction during platform operation at the X_1, Y_1, X_2, and Y_2 directions.

Direction	X_1	Y_1	X_2	Y_2
HMB Current(A)	0.67	0.73	1.46	2.58

In comparison, conventional active magnetic bearings typically employ a superposition of bias current and control current. For example, with a 5 A bias, the upper and lower coils in a single axis carry $(5 + I_c)$ and $(5 - I_c)$, respectively, where I_c is the dynamic control input. If it is assumed that the control current is 0, then in this control mode, the minimum power consumption of the magnetic bearing is about $P\approx86\ W$, which becomes larger when considering controlling the current. This setup leads to consistently high current magnitudes and elevated power consumption.

Since copper loss is approximately proportional to the square of the current, the hybrid design—by eliminating bias current through permanent magnet excitation—achieves a substantial energy-saving advantage. Experimental results indicate that the total power loss is reduced by over 90% compared to a typical bias-controlled AMB.

5. Conclusion

This paper proposed a novel 12-pole E-type tooth hybrid magnetic bearing (HMB) with low power consumption and high levitation accuracy. The structure features four symmetrically distributed E-type poles, effectively eliminating magnetic coupling between adjacent poles and enhancing flux efficiency. A sheet-shaped permanent magnet embedded in each main tooth provides bias magnetic flux, enabling efficient force generation with minimal coil current.

An equivalent magnetic circuit model was established, and finite element simulations verified the linearity of electromagnetic force and the absence of magnetic saturation under typical operating conditions. Experimental results further confirmed the feasibility of the design. In suspension and rotation experiments, the rotor remained stably levitated within ±15 μm displacement, and total power loss was reduced by over 90% compared to conventional AMBs.

The proposed HMB structure demonstrates excellent performance in compact, energy-sensitive applications such as kitchen ventilation systems and high-speed flywheel devices.

References

Allaire, P. E., Maslen, E. H., Lewis, D. W., & Flack, R. D. (n.d.). *Magnetic Thrust Bearing Operation and Industrial Pump Application*. https://doi.org/10.1115/94-GT-038

Garcia, R. F., Rolle, J. L. C., & Casado, M. H. (2009). Vibration attenuation control on HMBs. *2009 IEEE International Conference on Mechatronics*, 1–6. https://doi.org/10.1109/ICMECH.2009.4957152

Maslen, E. H., & Schweitzer, G. (Eds.). (2009). *Magnetic Bearings: Theory, Design, and Application to Rotating Machinery*. Springer Berlin Heidelberg. https://doi.org/10.1007/978-3-642-00497-1

Qinghai, W., Wei, N., Tao, Z., & Xiaoting, Y. (2011). Study on digital control system of AC 2-degree freedom HMB based on parameter automatic self-adjustment fuzzy PID. *2011 2nd International Conference on Intelligent Control and Information Processing*, *2*, 1098–1101. https://doi.org/10.1109/ICICIP.2011.6008423

Schweitzer, G. (1978). Ein aktives magnetisches Rotorlager- Auslegung und Anwendung / An active magnetic hub bearing—Design and application. *at - Automatisierungstechnik*, *26*(1–12), Article 1–12. https://doi.org/10.1524/auto.1978.26.112.10

Sun, J., Ju, Z., Peng, C., Le, Y., & Ren, H. (2017). A Novel 4-DOF Hybrid Magnetic Bearing for DGMSCMG. *IEEE Transactions on Industrial Electronics*, *64*(3), Article 3. https://doi.org/10.1109/TIE.2016.2626238

Wei, N., Qinghai, W., Defei, J., Xiaofeng, H., & Tao, Z. (2012). Study on measuring and control system of AC radial-axial hybrid magnetic bearing used in wind energy generation system. *Proceedings of the 31st Chinese Control Conference*, 6847–6850.

Ye, X., & Le, Q. (2020). Suspension Force Analysis on Novel Heteropolar Four Degrees of Freedom Hybrid Magnetic Bearing. *2020 IEEE International Conference on Applied Superconductivity and Electromagnetic Devices (ASEMD)*, 1–2. https://doi.org/10.1109/ASEMD49065.2020.9276327

Zhang, T., Le, Q., & Zhu, W. (2021). Structure and Suspension Force Analysis of Six-Pole Five Degrees of Freedom AC Hybrid Magnetic Bearing. *IEEE Transactions on Magnetics*, *57*(6), Article 6. https://doi.org/10.1109/TMAG.2021.3068860

Zheng, S., Li, H., Han, B., & Yang, J. (2017). Power Consumption Reduction for Magnetic Bearing Systems During Torque Output of Control Moment Gyros. *IEEE Transactions on Power Electronics*, *32*(7), Article 7. https://doi.org/10.1109/TPEL.2016.2608660

Zhou, L., & Li, L. (2016). Modeling and Identification of a Solid-Core Active Magnetic Bearing Including Eddy Currents. *IEEE/ASME Transactions on Mechatronics*, *21*(6), Article 6. https://doi.org/10.1109/TMECH.2016.2582644